Anal. Chem. **2002,** *74,* 5009−5016

High-Resolution TOF-SIMS Study of Varying Chain Length Self-Assembled Monolayer Surfaces

Kurt V. Wolf,[†] David A. Cole,[‡] and Steven L. Bernasek*,[†]

Department of Chemistry, Princeton University, Princeton, New Jersey 08544, and Evans East, East Windsor, New Jersey 08520

A high-resolution time-of-flight secondary ionization mass spectrometer (TOF-SIMS) has been used to investigate chain length effects in hydrocarbon self-assembled monolayer (SAM) surfaces on gold substrates. A wide range of *n*-alkanethiols was used to make homogeneous SAM surfaces, which included both odd and even hydrocarbon chain length thiols. Variations in coverage, extent of oxidation, and high-mass cluster formation as a function of hydrocarbon chain length of the alkanethiol SAM surfaces were investigated. Long−short chain length effects were observed for the relative coverage of the SAM surfaces, which directly influences the extent of oxidation for the thin films. The formation of gold−sulfur and gold−adsorbate cluster ions was also observed, since the mass range of the TOF-SIMS made it possible to monitor all of the cluster ions that were formed following the high-energy ion/surface interactions.

The technology of time-of-flight secondary ion mass spectrometry (TOF-SIMS) has improved dramatically in the past decade. Along with other methods such as X-ray photoelectron spectroscopy (XPS), Auger electron spectroscopy (AES), and infrared spectroscopy (IR), TOF-SIMS has become an indispensable tool for surface analysis.[1] In this paper, the use of a commercially available TOF-SIMS instrument to study self-assembled monolayer (SAM) surfaces is described. The SIMS ionization method when coupled with a time-of-flight mass analyzer allows for high mass resolution. This specific technique is able to detect low-mass fragments as well as ions with mass-to-charge ratios of thousands of atomic mass units with parallel detection of all ions for a given polarity. This process also has the ability to image surfaces, providing spatially resolved molecular information about the surface.[2]

The detailed molecular information that can be obtained from a mass spectrum makes static SIMS suitable for the analysis of organic surfaces when compared to dynamic SIMS.[3] Often when metallic substrates are used, cluster ions are detected in the secondary ion mass spectrum. Uniquely, when an organic thin film is deposited on a metallic surface, a combination of metal−metal, organic, and metal−organic cluster ions is formed.[4,5] Studying cluster formation using a well-characterized system such as SAM surfaces can increase our knowledge of high-energy ion/surface collisions.

The purpose of this study was to analyze the structure and composition of alkanethiol self-assembled monolayer surfaces as a function of chain length using the TOF-SIMS technique. A wide range of unmixed alkanethiols, $CH_3(CH_2)_nSH$, were used to form the thin films. Alkanethiols and disulfides self-assemble on Au (111) surfaces to form well-ordered monolayers, which are bound to the surface through a sulfur−gold bond.[6−10] In the standing-up phase, the backbone of the SAM surface, which is composed of the methylene groups of the alkyl chains, is oriented in an all-trans conformation with an overall chain tilt angle of ∼30° from the surface normal, as determined by ellipsometry and IR spectroscopy.[11,12] The TOF-SIMS technique can provide detailed information about the chemical composition of self-assembled monolayer systems.[13] This method makes use of the fact that positively and negatively charged ions are emitted from the surface upon ion bombardment and are readily detected by the time domain mass analyzer. The bombardment of the surface with the primary ion beam leads to the desorption of intact adsorbate ions as well as characteristic fragment ions. The reaction of secondary ions and neutrals during the collision cascade yields large cluster ions.[4]

Cluster ions of gold and gold−adsorbate species have been reported in the literature.[14,15] Nanoclusters of gold have been a

* Corresponding author. E-mail: sberna@princeton.edu. Fax: 609-258-1593.
[†] Princeton University.
[‡] Evans East.

(1) Schwieters, J.; Cramer, H. G.; Heller, T.; Jurgens, U.; Niehuis, E.; Zehnpfenning, J.; Benninghoven, A. *J. Vac. Sci. Technol. A* **1991**, *6*, 2864−2871.
(2) Aubriet, F.; Poleunis, C.; Bertrand, P. *J. Mass Spectrom.* **2001**, *36*, 641−651.
(3) Leufgen, K. M.; Rulle, H.; Benninghoven, A.; Sieber, M.; Galla, H. J. *Langmuir* **1996**, *12*, 1708−1711.
(4) Liu, K. S. S.; Yong, C. W.; Garrison, B. J.; Vickerman, J. C. *J. Phys. Chem. B* **1999**, *103*, 3195−3205.
(5) Harris, R. D.; Baker, W. S.; van Stipdonk, M. J.; Crooks, R. M.; Schweikert, E. A. *Rapid Commun. Mass Spectrom.* **1999**, *13*, 1374−1380.
(6) Nuzzo, R. G.; Fusco, F. A.; Allara, D. L. *J. Am. Chem. Soc.* **1987**, *109*, 2358−2368.
(7) Porter, M. D.; Bright, T. B.; Allara, D. L.; Chidsey, C. E. D. *J. Am. Chem. Soc.* **1987**, *109*, 3559−3568.
(8) Bain, C. D.; Troughton, E. B.; Tao, Y. T.; Evall, J.; Whitesides, G. M.; Nuzzo, R. G. *J. Am. Chem. Soc.* **1989**, *111*, 321−335.
(9) Vargas, M. C.; Giannozzi, P.; Selloni, A.; Scoles, G. *J. Phys. Chem. B* **2001**, *105*, 9509−9513.
(10) Nuzzo, R. G.; Allara, D. L. *J. Am. Chem. Soc.* **1983**, *105*, 4481−4483.
(11) Schreiber, F. *Prog. Surf. Sci.* **2000**, *65*, 151−256.
(12) Nuzzo, R. G.; Dubois, L. H.; Allara, D. L. *J. Am. Chem. Soc.* **1990**, *112*, 558−569.
(13) Fisher, G. L.; Walker, A. V.; Hooper, A. E.; Tighe, T. B.; Bahnck, K. B.; Skriba, H. T.; Reinard, M. D.; Haynie, B. C.; Opila, R. L.; Winograd, N.; Allara, D. L. *J. Am. Chem. Soc.* **2002**, *124*, 5528−5541.
(14) Wallace, W. T.; Whetten, R. L. *Eur. Phys. J. D* **2001**, *16*, 123−126.

10.1021/ac020275s CCC: $22.00
Published on Web 08/24/2002

topic of great interest for the scientific community due to their optical and electronic properties.[16] Colloidal gold nanoparticles in solution show a red color due to surface plasmon absorption. Adsorbate gold clusters, such as thiol-based adsorbates, have been shown to exhibit visible to infrared luminescence.[17] Link et al. showed the characteristics of the $Au_{28}(SG)_{16}$ cluster, where the ligands consisted of 16 tripeptide gluthathione units (Glu-Cys-Gly). A 1.3-eV absorption onset to the conduction band, corresponding to the HOMO−LUMO gap, produced a broad band of luminescence, which extended over the visible to the infrared region. A similar study showed that the Au_{28}−glutathione cluster system exhibited molecular properties.[18] This characteristic was largely due to the fact that half of the molecular weight of the cluster system stems from the capping ligands. This molecular behavior is different from larger gold nanoparticles, where the $Au_{28}(SG)_{16}$ cluster was characterized to have a wide range of luminescence with a long lifetime, while other nanoparticles consist of a single metal-enhanced luminescence that is relatively short-lived.[18]

Developing nanosize electrodes has also received significant attention in recent years.[19] Green et al. showed that a nanometer-size gold−thiolate electrode illustrated the characteristics of a capacitor. Studies of these three-dimensional monolayer systems showed that the nanoparticle electrode could be charged. A distinct alkanethiol chain length dependence was also observed, which showed that the cluster capacitance increased as the alkanethiol decreased in chain length. The synthesis and size determination of these three-dimensional SAM surfaces is well known.[20] The growth dynamics of the monolayer protected clusters has also been reported.[21] Clusters with a diameter of 1.5−5.2 nm, which corresponds to 100−4800 gold atoms/core, were reported to be largely metallic in nature.[20] It was shown that the alkanethiolate adsorbates stabilized the gold core, where 53−520 ligands were shown to attach as thiolates (not thiols), as determined by the thermolysis studies.

Mass spectrometry has been used previously to characterize clusters. Hemminger and co-workers used laser desorption mass spectrometry to study SAM surfaces.[22] They concluded that thiolates are formed on the Au surface. Air oxidants, such as sulfonates, are observed, with the shorter chain length SAM films showing a higher affinity for oxygen. The large dynamic range of time-of-flight mass analyzers makes them ideal for studying high-mass cluster ions, as documented by Vezmar et al..[15] These mass analyzers have been used to study high-mass cluster ions, with clusters as large as $Au_{140}S$ (27 609 amu) having been observed in these systems. With the use of a laser ablation technique, intense localized heating of the surface desorbs large pieces of the metallic substrate. Smaller gold−carbonyl clusters have also been reported using a similar technique.[14,23] It was shown that the gold clusters tend to be highly electronegative, which may explain their detection as negatively charged ions in many mass spectrometry measurements. The stability of the $Au_N(CO)_M$ clusters was studied by Wallace and Whetten.[23] The two-electron-donor system of CO showed an enhanced stabilization for negative ions when the gold electron subshell contained 8, 14, 18, and 20 electrons.[23]

Garrison and Winograd examined the dynamics of ion/surface scattering and the formation of metallic cluster ions.[24] Work has been carried out to understand the desorption processes of adsorbate material during secondary ion mass spectrometry. A recent article explains the dynamics of multilayer versus monolayer desorption processes.[24] It was observed that multilayers of benzene on Ag (111) desorb via an anion/surface collision cascade mechanism, such that adsorbate collisions by the substrate molecules initiates the desorption process. For a multilayer system, benzene desorbs from the surface of the multilayer with a lower kinetic energy than for the monolayer system, which is indicative of a series of chemical reactions.[24] Studies of the collision cascade for molecular solids and monitoring neutral molecules during SIMS have also been carried out.[25,26] TOF-SIMS has been used to study modified surfaces, where the terminal functional group of the SAM surface dictates the adsorption of vapor-deposited Al atoms.[27] For example, the OH-terminated SAM surface prevents the penetration of Al into the organic matrix, while the OCH_3-terminated surface permits the incorporation of Al into the matrix. Liu et al. carried out a detailed study of the dynamic processes that occur during high-energy ion/surface interactions with alkanethiol SAM surfaces.[4] This led to a theoretical understanding of the collision cascade and explained the formation of large mass clusters using molecular dynamics. Vickerman is also well known for using SIMS to characterize organic surfaces.[28] Reference spectra have been included in software programs to match unknown spectra with the use of a SIMS library, which includes these organic surfaces.

Even though SIMS has been used extensively to study SAM surfaces, many groups have overlooked the high-mass region of the mass spectra. Tarlov and Newman used static SIMS to study the oxidation of SAM surfaces.[29] They included a wide range of even chain length SAM surfaces; however, the $CH_3(CH_2)_{13}S$−Au surface was not included. This may have been due to an instrumental limit since they used a quadrupole mass analyzer, which would be unable to resolve the cluster ions for this surface since clusters with different integer values of gold, sulfur, and the intact thiolate all have similar masses. The $CH_3(CH_2)_{13}S$−Au SAM surface is included in our work and it tests the high-mass resolution of the TRIFT *(tri*ple *f*ocusing *t*ime-of-*f*light) design.

(15) Vezmar, I.; Alvarez, M. M.; Khoury, J. T.; Salisbury, B. E.; Shafigullin, M. N.; Whetten, R. L. *Z. Phys. D* **1997**, *40*, 147−151.
(16) de Heer, W. A. *Rev. Mod. Phys.* **1993**, *65*, 611−676.
(17) Link, S.; Beeby, A.; FitzGerald, S.; El-Sayed, M. A.; Schaaff, T. G.; Whetten, R. L. *J. Phys. Chem B* **2002**, *106*, 3410−3415.
(18) Link, S.; El-Sayed, M. A.; Schaaff, T. G.; Whetten, R. L. *Chem. Phys. Lett.* **2002**, *356*, 240−246.
(19) Green, S. J.; Stokes, J. J.; Hostetler, M. J.; Pietron, J.; Murray, R. W. *J. Phys. Chem. B* **1997**, *101*, 2663−2668.
(20) Hostetler, M. J.; Wingate, J. E.; Zhong, C. J.; Harris, J. E.; Vachet, R. W.; Clark, M. R.; Londono, J. D.; Green, S. J.; Stokes, J. J.; Wignall, G. D.; Glish, G. L.; Porter, M. D.; Evans, N. D.; Murray, R. W. *Langmuir* **1998,** *14*, 17−30.
(21) Chen, S.; Templeton, A. C.; Murray, R. W. *Langmuir* **2000,** *16*, 3543−3548.
(22) Li, Y.; Huang, J.; McIver Jr., R. T.; Hemminger, J. C. *J. Am. Chem. Soc.* **1992**, *114*, 2428−2432.
(23) Wallace, W. T.; Whetten, R. L. *J. Phys. Chem, B* **2000**, *104*, 10964−10968.
(24) Winograd, N.; Garrison, B. J. *Int. J. Mass Spectrom.* **2001**, *212*, 467−475.
(25) Krantzman, K. D.; Postawa, Z.; Garrison, B. J.; Winograd, N.; Stuart, S. J.; Harrison, J. A. *Nucl. Instrum. Methods Phys. Res. B* **2001**, *180*, 159−163
(26) Postawa, Z.; Meserole; Cyganik, P.; Szymonska, J.; Winograd, N. *Nucl. Instrum. Methods Phys. Res. B* **2001**, *182*, 148−154.
(27) G. L. Fisher, A. V. Walker, A. E. Hooper, T. B. Tighe, K. B. Bahnck, H. T. Skriba, M. D. Reinard, B. C. Haynie, R. L. Opila, N. Winograd, D. L. Allara. *J. Am. Chem. Soc.* **2002**, *124*, 5528−5541.
(28) Vickerman, J. C.; Briggs, D.; Henderson, A. *The Static SIMS Library*; Surface Spectra Ltd.: Manchester, U.K., 1997.
(29) Tarlov, M. J.; Newman, J. G. *Langmuir* **1992**, *8*, 1398−1405.

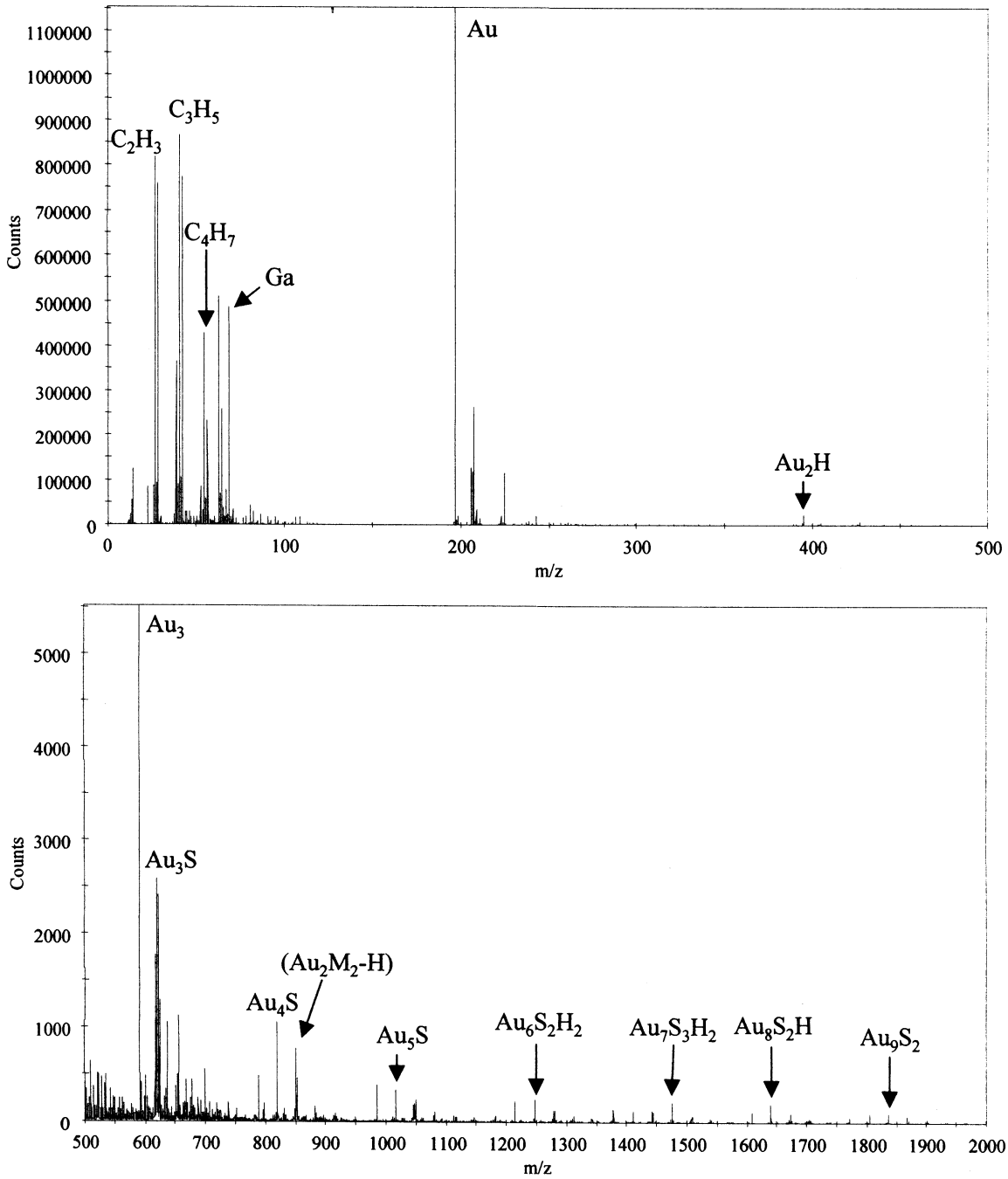

Figure 1. Positive mass spectra for the $CH_3(CH_2)_{13}S-Au$ SAM surface.

When compared to the laser desorption techniques, static SIMS will not be able to produce such high-mass cluster ions; however, the dynamics are quite different as the effects of intense localized heating will be drastically decreased. The work presented here introduces the large cluster ions that are formed via the SIMS process on homogeneous unmixed SAM surfaces. It also illustrates the semiquantitative nature of static SIMS in relative coverage and oxidation studies characteristic for the range of SAM surfaces examined.

MATERIAL AND METHODS

Materials. Eight varying chain length SAM surfaces ($CH_3(CH_2)_nS-Au$, where n = 10, 11, 12, 13, 14, 15, 16, and 17) were used in these studies. Seven thiols ($CH_3(CH_2)_nSH$, where n = 10, 11, 12, 13, 14, 15, and 17) were purchased in pure form commercially from Aldrich, TCI, and Pfaltz & Bauer, Inc. and used without further purification. The $CH_3(CH_2)_{16}S-Au$ SAM surface was prepared from a mixture of $CH_3(CH_2)_{16}SH$ and $(CH_3(CH_2)_{16}S)_2$, which was obtained from Professor David Allara at the Pennsylvania State University. The starting materials were monitored for purity using high-resolution nuclear magnetic resonance and mass spectrometry. No evidence of oxidized product impurities was observed. A problem concerning the purity of the $CH_3(CH_2)_{12}SH$ thiol was noticed. NMR indicated that this thiol was contaminated by impurities that appeared to be other thiol molecules. Mass spectrometry confirmed the NMR findings and also showed that the solution did not contain any alkanethiol

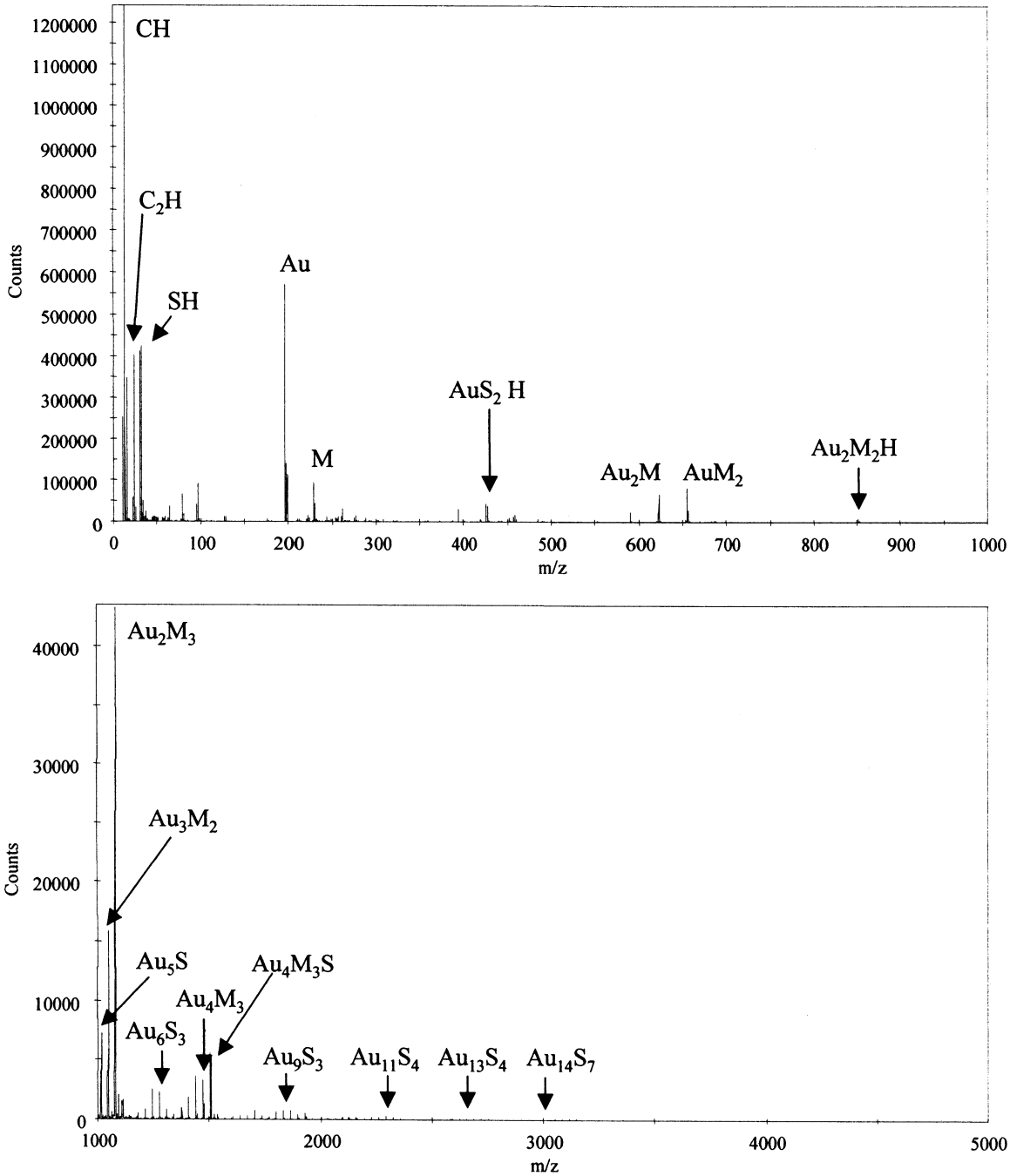

Figure 2. Negative mass spectra for the $CH_3(CH_2)_{13}S-Au$ SAM surface.

chains that were longer than the $CH_3(CH_2)_{12}SH$ thiol. This thiol could not be purified through distillation, and the large boiling temperature range indicted possible branched thiols as contaminants. Results for this surface should be noted with this caveat.

Gold Substrate. All SAM surfaces were formed on vapor-deposited gold substrates purchased from Evaporated Metal Films of Ithaca, NY. The substrates consist of 1000 Å of vapor-deposited Au on 50-Å Ti deposited on silica glass slides with surface dimensions of $^{11}/_{16}$ in. × $^{17}/_{32}$ in. The Au surfaces were precleaned using a reducing hydrogen flame. The gold substrates were flame treated for a few seconds followed by an air-cooling lapse of a few seconds. This process was continued for 10 cycles.

Monolayer Preparation. Self-assembled monolayer surfaces were prepared by immersing a freshly cleaned Au substrate into a 1 mM alkanethiol/absolute ethanol solution. Each surface was permitted to grow in a single thiol solution for at least two weeks in order for the packing of the thin film to fully equilibrate. Each solution was prepared from one specific chain length thiol, and no mixed films were prepared. The SAM surfaces were rinsed five times with absolute ethanol. The surfaces were attached to the sample holder and pumped down to UHV conditions.

Instrumentation. The mass spectra were obtained using a Physical Electronics TFS-2000 TOF-SIMS. The system contains a gallium liquid metal ion source (LMIS). This source is capable of producing a subnanosecond pulsed beam of gallium primary ions which is focused on the sample producing secondary ions from the target surface. The primary ion pulse initiates the timing

of the TOF process and was then bunched and rastered over the sample surface.

A preset potential on the surface accelerates the secondary ions into the extraction optics through a high-mass blanker. For a predetermined time, the potentials on the two plates of the mass blanker are set equal; this sets the lower and upper mass limits for the secondary ions. The system contains a secondary electron detector (SED), which is used to tune the primary ion beam and can also be applied for ion-induced electron microscopy (IIEM). The secondary ions enter the TRIFT mass analyzer and pass through an angular filter and three electrostatic sector analyzers (ESAs). This design allows the 2-m flight tube to be oriented in a semicircular path, where the secondary ion beam is bent by the three electrostatic sector analyzers. The ions exit the final ESA and are detected using an electron multiplier. The mass spectrum is then determined from the time domain by the predetermined physical constants of the instrument, where the final calibration is carried out through the assignment of known mass fragments for a given spectrum. The system also contains an electron flood gun to eliminate unwanted sample charging.

Nine surfaces, eight SAM surfaces and one gold blank, were investigated from mass 1.5 to 5000 amu for negative secondary ions and from mass 0.5 to 2000 amu for positive ions. The bunched primary gallium ion beam, with an energy of 12 keV for positive ion ejection and 18 keV for negative ion ejection, was rastered over a 40.3 μm × 40.3 μm area, and each spectrum was acquired over a total time interval of 15 min. The mass resolution for gold, $m/\Delta m$, throughout the study remained constant with a value of 8000. The total dose of the primary ions impinging on the surface was 1.7×10^{13} Ga^+ ions/cm^2.

RESULTS AND DISCUSSION

The positive and negative ion mass spectra consist of a wide range of species as seen in Figures 1 and 2. Classical hydrocarbon fragmentation patterns, inferred from the spectra, are observed for the self-assembled monolayers, in addition to the evident formation of high-mass gold−adsorbate (Au_xM_y) and gold−sulfur (Au_mS_n) cluster ions. These cluster ions were observed previously by several other groups.[22,28,30] When comparing the negative mass spectra with the positive mass spectra, it is apparent that the negative spectrum contains a greater number of gold−adsorbate and gold−sulfur peaks. Table 1 summarizes data for the largest adsorbate clusters, defined as any cluster with at least one intact thiolate molecule (M), and the largest nonadsorbate clusters, any cluster that does not contain an intact thiolate molecule. These data are shown for the eight SAM surfaces and the clean Au substrate. Hemminger's group demonstrated using laser desorption/ionization mass spectrometry that the adsorbates desorb from SAM surfaces as anions.[22] Whetten showed that gold clusters are very electronegative and that gold cluster ions with two-electron-donor adsorbates showed enhanced stabilization with 18 electron configurations.[23] Therefore, the observation of gold−sulfur-containing cluster anions, such as AuS^-, could also be explained by this 18-electron configuration. Perhaps it is this enhanced stabilization, along with the presence of a thiolate on the SAM surfaces, that causes the high-mass cluster ions to be more anionic, rather than cationic, in nature.

Table 1. The Largest Adsorbate and Nonadsorbate Clusters Observed for the SAM Surfaces

surface	mass (amu)	fragment
	Adsorbate Clusters	
$CH_3(CH_2)_{17}S-Au$	1731.95	$Au_3M_4^-$
$CH_3(CH_2)_{16}S-Au$	2069.82	$Au_5M_4^-$
$CH_3(CH_2)_{15}S-Au$	2013.75	$Au_5M_4^-$
$CH_3(CH_2)_{14}S-Au$	2003.94	$Au_4M_5^-$
$CH_3(CH_2)_{13}S-Au$	2327.79	$Au_6M_5^-$
$CH_3(CH_2)_{12}S-Au$	1845.57	$Au_5M_4^-$
$CH_3(CH_2)_{11}S-Au$	2187.64	$Au_6M_5^-$
$CH_3(CH_2)_{10}S-Au$	2501.68	$Au_7M_6^-$
	Nonadsorbate Clusters	
$CH_3(CH_2)_{17}S-Au$	3114.36	$Au_{15}S_5^-$
$CH_3(CH_2)_{16}S-Au$	3114.36	$Au_{15}S_5^-$
$CH_3(CH_2)_{15}S-Au$	3146.33	$Au_{15}S_6^-$
$CH_3(CH_2)_{14}S-Au$	3114.36	$Au_{15}S_5^-$
$CH_3(CH_2)_{13}S-Au$	3604.21	$Au_{17}S_8^-$
$CH_3(CH_2)_{12}S-Au$	3572.24	$Au_{17}S_7^-$
$CH_3(CH_2)_{11}S-Au$	4881.92	$Au_{23}S_{11}^-$
$CH_3(CH_2)_{10}S-Au$	4881.92	$Au_{23}S_{11}^-$
Au	3348.43	Au_{17}^-

The formation of high-mass cluster ions, like those reported in Table 1, has not been studied as a function of chain length prior to this time. The formation of gold cluster ions up to Au_{17}^- for the blank gold sample (i.e., a substrate with no alkanethiol adsorbate) allows for a standard to compare with the adsorbate gold cluster ions shown in Table 1. The addition of sulfur to the gold clusters, forming Au_mS_n cluster ions, should stabilize the system, as was seen previously in the work of Whetten[15,31] and Murray.[20,21] A distinction can be made for the long- versus short-chain SAM surfaces. The shorter chain SAM surfaces allow for larger cluster ions to be formed. Table 1 shows that the nonadsorbate gold cluster ions observed for the short-chain SAM surfaces are larger than the Au_{17}^- maximum observed for the bare gold substrate, where Au_mS_n cluster ions are formed where m is greater than or equal to 17. The adsorbate cluster ions, Au_xM_y, also show a similar chain length dependence for their formation. This distinct long−short chain length effect could be explained by an increase in chain/chain interactions as the alkanethiol chain length is increased, thus limiting the extent of cluster formation during the ion/surface interactions. The total ion yield remained fairly constant with a slight decrease as the chain length of the thiol on gold was increased. This is consistent with a uniform dissociation process, meaning that the longer chain length thin films do not dissociate more than the shorter chain length films. This idea is confirmed by a plot of (CH_3^+/total ion yield) versus the chain length of the alkanethiol on gold, where no chain length dependence was observed. A more quantitative discussion of the dynamics of cluster formation as a function of chain length will be presented in a future publication.[32]

Although over 3000 peaks have been identified from the mass spectra of the eight self-assembled monolayer surfaces, the $CH_3(CH_2)_{13}S-Au$ SAM surface proved to be the most challenging to mass resolve the cluster peaks. Different cluster ions with varying integer values of gold, intact thiolate, sulfur, or hydrogen all have very similar masses, as can be seen in Figure 3. The high mass

(30) Offord, D. A.; John, C. M.; Linford, M. R.; Griffin, J. H. *Langmuir* **1994**, *10*, 883−889.

(31) Wang, Z. L.; Harfenist, S. A.; Whetten, R. L.; Bentley, J.; Evans, N. D. *J. Phys. Chem. B* **1998**, *102*, 3068−3072.

(32) Wolf, K. V.; Cole, D. A.; Bernasek, S. L. Submitted to *J. Phys. Chem. B.*

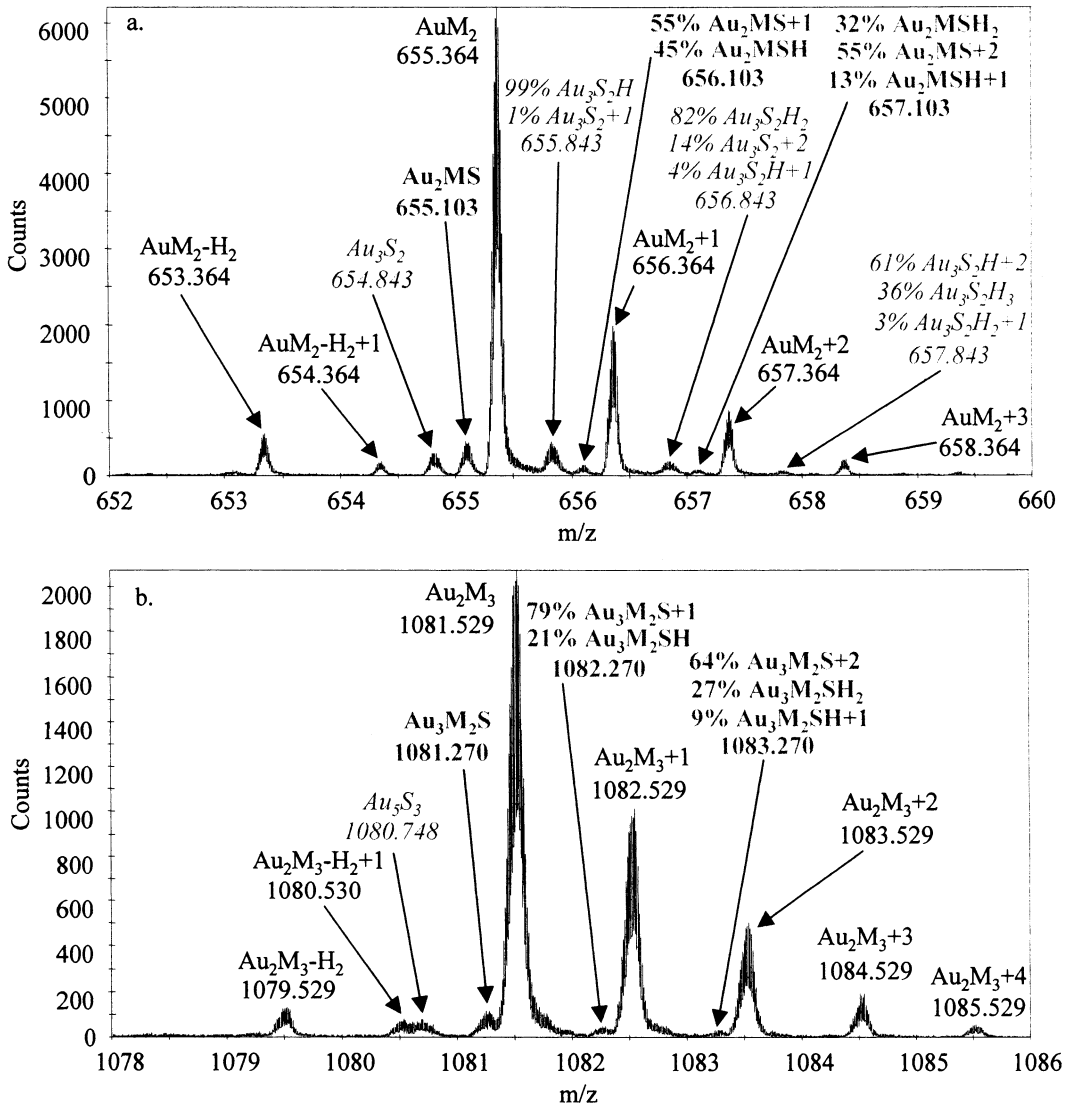

Figure 3. High-resolution negative mass spectra of a $CH_3(CH_2)_{13}S-Au$ SAM surface. Note the percentages report the compositional fraction for a given peak, where cluster ions reported as +1, +2, +3, etc., correspond to the appropriate isotopic ion (e.g., AuM_2+1 = the +1 isotope for the AuM_2 cluster ion).

resolution of the TRIFT design allowed distinct peak separation of cluster ions with a mass difference as low as 0.22 amu for the spectrum shown in Figure 3b. Comparing panels a and b of Figure 3, an obvious peak broadening is observed with increasing mass. This phenomenon was expected since the full width at half-maximum for a given peak using a TOF mass analyzer is proportional to the mass-to-charge ratio.

With the careful use of known isotope ratios, a detailed assignment of peaks was made for the spectra as illustrated in Figure 3. The base peak of Figure 3a gives rise to the conformation of $AuM_2 + 1$, $AuM_2 + 2$, and $AuM_2 + 3$ isotope ions (i.e., the $AuM_2 + 1$ is defined as the +1 isotope for the AuM_2 cluster ion) with no sign of hydrogenation. However, the sulfur-rich adsorbate cluster ions ($Au_aM_bS_c$) and the nonadsorbate cluster ions (Au_mS_n) show a stronger affinity for hydrogen, as illustrated in Figure 3. Therefore, the formation of the sulfur-dominated cluster ions appears to be stabilized by the addition of hydrogen. Figure 3b reconfirms this hypothesis with similar chemistry seen for the heavier cluster ions.

The formation of the SAM surfaces and their uniform coverage was demonstrated earlier using X-ray photoelectron spectroscopy (XPS).[33] TOF-SIMS allows the examination of uniformity of coverage on a much smaller length scale, micrometers rather than millimeters typical of XPS. This technique allows the uniformity of coverage to be directly measured. Imaging the SAM surfaces over multiple positions of the sample provided a means to determine whether the surfaces were homogeneously covered. The surface images for the $CH_3(CH_2)_{10}S-Au$ and $CH_3(CH_2)_{11}S-Au$ SAM surfaces were examined and appeared to be quite homogeneous for any specific imaging point of the surface. At no time was a bare gold region observed for the thin films.

Although the images of the SAM surfaces illustrate a uniform coverage, they do not provide a quantitative measurement of the coverage. A plot of total equivalents of sulfur in the sulfur-containing ion peaks divided by the total equivalents of gold in the gold-containing peaks in the mass spectra provides a manner to compare the surface coverage for each SAM surface. This

(33) Wolf, K. V.; Cole, D. A.; Bernasek, S. L. *Langmuir* **2001**, *17*, 8254−8259.

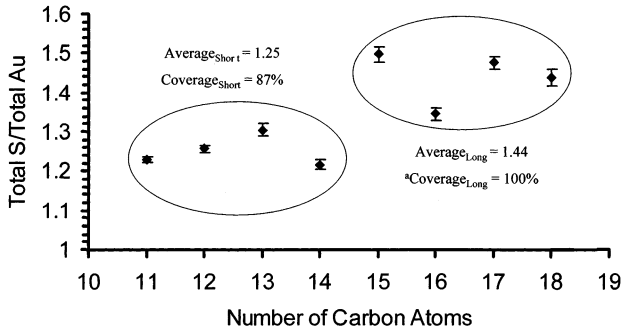

Figure 4. Quotient of the total equivalents of sulfur-containing ions and the total equivalents of Au-containing ions versus the total number of carbon atoms in the alkanethiol. The error bars represent plus or minus two standard deviations based on the propagated error for the peaks in the mass spectra. ^{a}Coverage$_{Long}$ assumed the coverage of the long-chain SAM surfaces was 100%

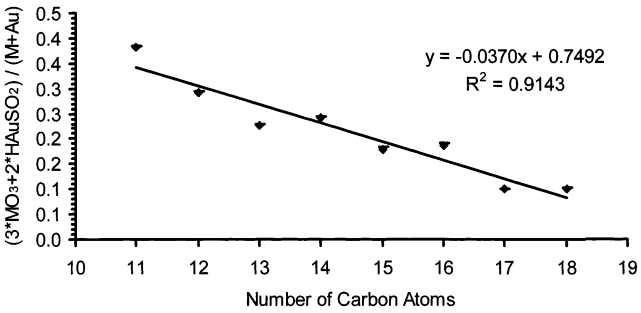

Figure 5. Equivalent oxidation of the SAM surface versus the number of carbon atoms in the alkanethiol. The error bars represent plus or minus two standard deviations based on the propagated error for the peaks in the mass spectra.

information is shown in Figure 4. It is important to note that the quotient plotted on the *y*-axis obviously does not represent the absolute coverage of the thin films. This is due to differences in electron affinity, fragmentation pathways, and neutralization mechanisms for the individual ions formed. However, it should be safe to assume that these processes will be constant from surface to surface over the range of thin films studied, since the total ion yield does not vary drastically, as described earlier. Therefore, information pertaining to the relative coverage from surface to surface can be obtained, which allows the self-assembled monolayer surfaces to be compared. The coverage of SAM surfaces has been previously studied and a long−short chain length effect was observed.[6] This effect was confirmed in this work and allowed for a standard to compare the results of the SIMS data. Figure 4 shows a slight increase in the equivalent coverage as the chain length of the alkanethiol chemisorbed to gold is increased with a distinct discontinuity occurring between the $CH_3(CH_2)_{13}S-Au$ and the $CH_3(CH_2)_{14}S-Au$ SAM surfaces. Again, a long−short chain length effect is apparent. If the equivalent coverages measured in this manner for the short-chain alkanethiol SAM surfaces ($\leq CH_3(CH_2)_{13}S-Au$) are averaged, a value of 1.25 is obtained. Likewise, when the equivalent coverage for the long-chain SAM surfaces ($> CH_3(CH_2)_{13}S-Au$) are averaged, a mean value of 1.44 is found. If the long hydrocarbon chain surfaces are assigned an actual coverage of 100%, then the short-chain SAM surfaces would correspond to a coverage of 87%. These values agree very well with previous coverage studies where the coverage of long- and short-chain SAM surfaces was determined to be 99% and 90%, respectively.[6,11]

The final chain length effect that will be discussed is the extent of oxidation. Figure 5 shows the magnitude of oxidation for the self-assembled monolayer surfaces where the quotient of the *y*-axis is similar to that used by Offord et al..[30] In this case, the dominant oxidized peaks (where a degree of oxidation had occurred) were divided by the sum of their appropriate nonoxidized ions, where the stoichiometric values for oxygen are used in the numerator. A linear least-squares fit, with good correlation, depicts that the extent of oxidation decreases as the chain length of the alkanethiol increases. This chain length effect was observed before by several groups; however, in past cases, the odd-chain-length SAM surfaces were ignored whereas in this study they are included.[22,29,30] The extent of oxidation appears to be limited by the longer chain alkanethiol tails since as the thickness of the thin film is increased, the diffusion and permeability of atmospheric oxidants would be diminished. The extent of oxidation increases for the short-chain SAM surfaces since the shorter chains appear to have a slightly lower coverage. Since Figure 4 shows the shorter chains have a lower relative packing, it seems clear that the effect of oxidation witnessed in Figure 5 could be directly related to the coverage of the organic thin films. Gauche defects in the shorter alkanethiol chains could cause the adsorbates to pack with a slightly lower coverage, which would result in larger gaps between the chains of the thin films resulting in greater diffusion of oxidants. The number of defects should, however, be small since the orientation of the terminal methyl group is macroscopically well-ordered for the thin films.[33] However, coverage cannot be the only factor controlling the extent of oxidation for the SAM surfaces. This is clear when Figures 4 and 5 are closely compared. The $CH_3(CH_2)_{14}S-Au$ SAM surface appears to have the largest relative coverage, but it is not the most inert surface in terms of oxidation. Since Figure 5 shows a very good linear fit to the data, film thickness must also contribute to the extent of oxidation, resulting in a larger number of steric hindrances for the oxidants to overcome, which would limit the diffusion of the oxidizing material. Examining Figure 5 closely, a slight step function is observed, where the odd-chain-length SAM surfaces seem to show a greater resistance to oxidation. This effect is quite interesting and could be attributed to the odd−even chain length effect concerning the orientation of the terminal methyl groups.[33] Since both the coverage and chain length of the thin films dictates the extent of oxidation, it was concluded that the S-terminus is the dominant site for oxidation, even though oxidized hydrocarbon fragments (with no sulfur atom present) were also observed in limited yields.

CONCLUSIONS

TOF-SIMS proved to be a very useful method for analyzing SAM surfaces. Its capabilities in imaging and its high mass resolution enabled chain length effects to be readily monitored. Also, the high-mass range of the TOF mass analyzer allowed for the observation of all possible cluster ions, where spectra for both positive and negative ions were obtained for high mass-to-charge ratios until no appreciable ion yield was detected. Static SIMS has some limitations for quantitative studies; however, in this study, TOF-SIMS was successfully used to compare varying chain length self-assembled monolayer surfaces. Varying the chain length of

the hydrocarbon backbone for the alkanethiols on gold proved to influence the thin films in both packing and stability. The stability of the SAM surfaces was observed by measuring the extent of oxidation in the thin films. The extent of oxidation showed a direct correlation with the relative coverage for the thin films. Gauche defects, for the SAM surfaces in the varying range of chain lengths studied here, may result in fluctuations in the coverage of the long- versus short-chain-length SAM surfaces. Therefore, the extent of oxidation appears to be affected mostly by the relative coverage and the overall thickness of the SAM surfaces. Since chain length effects dictate the amount of oxidation, it was concluded that the sulfur terminus of the alkanethiol is the dominant site of oxidation.

ACKNOWLEDGMENT

We thank Dr. Xia Dong for her assistance and advice for the SIMS analyses and Professor David Allara for material to produce the $CH_3(CH_2)_{16}S$-Au SAM surfaces, and we are grateful for the support of this work by the National Science Foundation, Division of Chemistry.

Received for review April 26, 2002. Accepted June 19, 2002.

AC020275S